Photocatalytic property of Zn-modified bismuth titanate

W. Feng Yao [a,*], Hong Wang [a], S. Xia Shang [b], X. Hong Xu [a],
X. Na Yang [a], Y. Zhang [a], Min Wang [a]

[a] *State Key Laboratory of Crystal Materials, Shandong University, Jinan, Shandong 250100, PR China*
[b] *Department of Environment Engineering, Shandong University, Jinan, Shandong 250100, PR China*

Abstract

Bismuth titanate with 1 at.% Zn modifications were fabricated by a chemical solution decomposition (CSD) method, and pure phase of $(Bi_{0.99}Zn_{0.01})_{20}TiO_{32}$ was first prepared at low sintering temperature of $400\,^\circ\text{C}$. As sintered at high temperature, the phase direct transformation between $(Bi_{0.99}Zn_{0.01})_{20}TiO_{32}$ and $(Bi_{0.99}Zn_{0.01})_4Ti_3O_{12}$ was observed. Their photocatalytic activities were also evaluated using methyl orange as a model organic compound. The photocatalytic degradation rate of methyl orange on $(Bi_{0.99}Zn_{0.01})_{20}TiO_{32}$ is faster than that on $(Bi_{0.99}Zn_{0.01})_4Ti_3O_{12}$ and $Bi_4Ti_3O_{12}$.
© 2002 Elsevier Science B.V. All rights reserved.

Keywords: Photocatalyst; Bismuth titanate; Doped; CSD

1. Introduction

Recently much interest has been paid to photocatalytic methods, because they provide a promising strategy for cleaning polluted air or water. TiO_2 is known to be one of the most effective photocatalysts for the degradation of organic pollutants, and its photocatalytic behavior has been studied extensively [1–3]. Although titanium oxide catalysts are capable of decomposing a wide variety of oxide and inorganic pollutants and toxic materials, in both liquid and gas phase systems [2–6], yet their reactivity and selectivity are not enough for large-scale applications. It is, therefore, of interest to develop new photocatalysts with high photocatalytic properties. In the past decades, bismuth titanate had attracted much interest because

it has many applications in the field of microelectronics, electro-optics and dielectrics [7,8]. Several phases in Bi–Ti–O system are known, including $Bi_4Ti_3O_{12}$, $Bi_2Ti_2O_7$, $Bi_2Ti_4O_{11}$, $Bi_{12}TiO_{20}$, $Bi_{20}TiO_{32}$ and so on. In an earlier study the author has found that $Bi_4Ti_3O_{12}$ is a new photocatalyst showing high activity to photodegrade the 10 mg/l methyl orange solution in 4 h. But the photocatalytic activity of $Bi_4Ti_3O_{12}$ crystals still needs improving, because under similar conditions pure anatase TiO_2 prepared by us shows a higher photocatalytic property to photodegrade the aqueous methyl orange in 2.5 h. It is known that transition metal ions doped into catalysts can increase the quantum efficiency of the heterogeneous photocatalytic property by altering the e^-/h^+ pair recombination rate and promoting the interfacial charge transfer rates of photogenerated carriers [9–12]. So it is of interest to investigate the influence of metal nanoparticle deposition on the photocatalytic property of $Bi_4Ti_3O_{12}$. In the present paper, Zn^{2+} ions were doped

* Corresponding author. Tel.: +86-531-8564204;
fax: +86-531-8565403.
E-mail address: weifengyao@icm.sdu.edu.cn (W.F. Yao).

into bismuth titanate crystals by the chemical solution decomposition (CSD) method, and photocatalytic properties of as-prepared samples were evaluated using methyl orange as a model organic compound.

2. Experimental

The precursor materials of Zn-doped bismuth titanate crystals were prepared by a chemical solution decomposition method to give a doping level of 1 at.%. The dopant concentrations mentioned in this work are the nominal atomic concentration, which is based upon the assumption of quantitative incorporation of the dopant. Bismuth nitrate ($Bi(NO_3)_3 \cdot 5H_2O$), titanium butoxide ($Ti(OC_4H_9)_4$) and zinc acetate ($Zn(CH_3COO) \cdot 2H_2O$) were selected as starting materials, glacial acetic acid (CH_3COOH) was used as a solvent. Bismuth nitrate and the stoichiometric amount of zinc acetate were initially dissolved in CH_3COOH, and then titanium butoxide was added drop-wise with constant stirring. The formed solution was diluted with 2-methoxyethanol (CH_3OCH_2OH) to adjust its viscosity and surface tension. Dust and impurities were removed by filtering through 0.2 μm syringe filters. To keep the solution stable longer, a certain amount of acetylacetone ($C_5H_8O_2$) was added to the solution. After being stirred for 0.5 h by a magnetic stirrer, the solution was dried at 100 °C to remove the solvents and some organic materials. Then the obtained powder was calcined at higher temperature for 10 min to remove other organic materials and produce crystallinity. X-ray powder diffraction patterns of the prepared samples were carried out on a Rigaku D/MAX-γ X-ray diffractometer. The grain sizes in the powders are about 20–90 nm, as determined by transmission electron microscope measurements (Hitachi H-800 at 100 kV).

Photocatalytic activity of as-prepared samples was examined by the photo-decolorization of aqueous methyl orange. The primary step in photocatalysis process is the generation of electrons and holes within the catalyst particles. Then in the presence of dissolved oxygen and an electron donor, $^\bullet OH$ and O_2^- are formed. Methyl orange is attacked by the formed hydroxyl radicals and generates organic radicals or some other intermediates. Eventually all the parent compounds and intermediates are oxidized into CO_2,

SO_4^{2-} and NO_3^- [13,14]. The photodecolorization of aqueous methyl orange was carried out in a 150 ml Pyrex glass vessel with magnetic stirring. A 20 W UV lamp with a maximum emission at about 360 nm was used as the light source. Each as-prepared samples of different quality were suspended in 50 ml methyl orange aqueous solution (10 mg/l). The distance between the liquid surface and the light source was 5 cm, and the averaged intensity of UV irradiance was about 0.936 mW/cm^2 measured by an UV-Vis spectrophotometer. The concentrations of aqueous methyl orange were determined as a function of illumination time by measuring the absorbance at 464 nm with an UV-Vis spectrophotometer. The linear relationship between the absorbance at 464 nm (A) and the concentration of methyl orange (C) can be represented empirically by the equation: $A = 0.0727C$ [13].

3. Results and discussion

3.1. Characterization of as-prepared samples

The crystallization of bismuth titanate is influenced by many factors, such as annealing temperature, heating rate and so on. Annealing temperature is regarded as the most important factors. Fig. 1 shows the XRD patterns of as-prepared samples annealed in air from 400 to 950 °C for 10 min. The prepared samples exhibited a well-crystallized tetragonal phase of $(Bi_{0.99}Zn_{0.01})_{20}TiO_{32}$ at an annealing temperature of 400 °C for 10 min, the X-ray diffraction patterns of which were indexed based on tetragonal lattice as reported previously. According to Joint Committee of Powder Diffraction Standard data cards (42-202), most of the peaks emerged but a little one marked as (●) belong to $(Bi_{0.99}Zn_{0.01})_{20}TiO_{32}$ phase. This little peak, as shown in Fig. 1, increases with the rise of calcining temperature. Although the patterns of $(Bi_{0.99}Zn_{0.01})_{20}TiO_{32}$ did not show any significant variation when the annealing temperature roses to 500 °C, the little peak marked as (●) increases remarkably. As the annealing temperature increases to 600 °C, there exist two mixed phases $(Bi_{0.99}Zn_{0.01})_{20}TiO_{32}$ and $(Bi_{0.99}Zn_{0.01})_4Ti_3O_7$ in the prepared samples. The peaks of $(Bi_{0.99}Zn_{0.01})_{20}TiO_{32}$ become weaker, while that of $(Bi_{0.99}Zn_{0.01})_4Ti_3O_7$ phase marked as (●) increases. As shown in Fig. 1
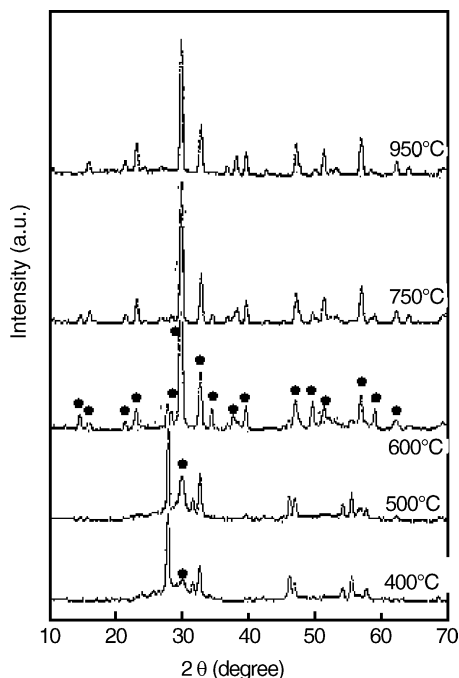
Fig. 1. XRD patterns of the 1 at.% Zn-doped bismuth titanate annealed in air from 400 to 950 °C for 10 min.

when the annealing temperature roses to 750 °C, the peaks of $(Bi_{0.99}Zn_{0.01})_{20}TiO_{32}$ phase disappear completely and the prepared samples possess the major phases of $(Bi_{0.99}Zn_{0.01})_4Ti_3O_7$ crystals. Similar results were found in the preparation of pure $Bi_2Ti_2O_7$ nanocrystals [15]. $Bi_{20}TiO_{32}$ was examined as a metastable phase and can transform gradually into the $Bi_2Ti_2O_7$ phase with the annealing time increasing at a temperature of 550 °C. Comparing the change of peaks of $(Bi_{0.99}Zn_{0.01})_{20}TiO_{32}$ with that of $(Bi_{0.99}Zn_{0.01})_4Ti_3O_7$ phase, it can be concluded that $(Bi_{0.99}Zn_{0.01})_{20}TiO_{32}$ is a metastable phase during the formation of $(Bi_{0.99}Zn_{0.01})_4Ti_3O_7$ and it can transforms gradually into the $(Bi_{0.99}Zn_{0.01})_4Ti_3O_7$ phase with the increase of annealing temperature.

Tetragonal bismuth titanate of $Bi_{20}TiO_{32}$ is an unstable phase in Bi–Ti–O system. According to the conventional phase diagram of Bi_2O_3–TiO_2 system, $Bi_{20}TiO_{32}$ phase cannot emerge at a low temperature of 400 °C. From Joint Committee of Powder Diffraction Standard data cards (42-202), pure phase of $Bi_{20}TiO_{32}$ crystals was prepared by Troemel et al.

through melting oxides at 1000 °C for 2 min and quenching at room temperature. But to the authors knowledge, there was no report about the preparation of pure $Bi_{20}TiO_{32}$ by the chemical solution method, because when the composition of Bi and Ti is Bi:Ti > 10:1, $Bi_{12}TiO_{20}$ phase but not $Bi_{20}TiO_{32}$ is easy to obtain [15,16]. The experimental results show that Zn ions doped can facilitate the formation of $(Bi_{0.99}Zn_{0.01})_{20}TiO_{32}$ and stabilize the phase structure. It is noteworthy that no pyrochlore phase of $(Bi_{0.99}Zn_{0.01})_2Ti_2O_7$ emerged in the formation process of $(Bi_{0.99}Zn_{0.01})_4Ti_3O_7$ crystals. $Bi_2Ti_2O_7$ is regarded as a metastable phase during $Bi_4Ti_3O_{12}$ formation. In the preparation of La modified bismuth titanate ceramics, Jiang et al. [17] pointed out that $Bi_2Ti_2O_7$ is an unstable phase during $Bi_4Ti_3O_{12}$ formation, and the phase structure can be stabilized by ionic modification. Hou et al. [15] showed that $Bi_{20}TiO_{32}$ was a metastable phase during $Bi_2Ti_2O_7$ formation. So the $Bi_{20}TiO_{32}$ can be also regarded as one metastable phase in the formation process of $Bi_4Ti_3O_{12}$ phases. Although the direct transform between $(Bi_{0.99}Zn_{0.01})_{20}TiO_{32}$ and $(Bi_{0.99}Zn_{0.01})_4Ti_3O_7$ phases is not clear at the present stage, while it can be deduced that the disappearance of the pyrochlore bismuth titanate is something with the dopant Zn^{2+} ions.

3.2. Photocatalytic activity of the prepared samples

The UV-Vis for methyl orange in distilled water show two absorption maxima (Fig. 2). The first band observed at 270 nm and the second band at 464 nm. The band at 464 nm was used to monitor the effect of the photocatalysis on the degradation of methyl orange.

Figs. 3 and 4 show the absorption spectra of methyl orange solution at different times following the photocatalystic degradation. The decreases in the absorbance band at 464 nm reflect the disappearance of methyl orange as it gets oxidized at the active site on the catalyst. No decolorization occurs in the absence of light when the catalyst is present. Further more the concentration of methyl orange decreased negligibly over the time span of these experiments in the absence of photocatalysts. The dependence of the photodegradation activity on the concentration of the catalysts calcined at 600 °C for 10 min was studied.
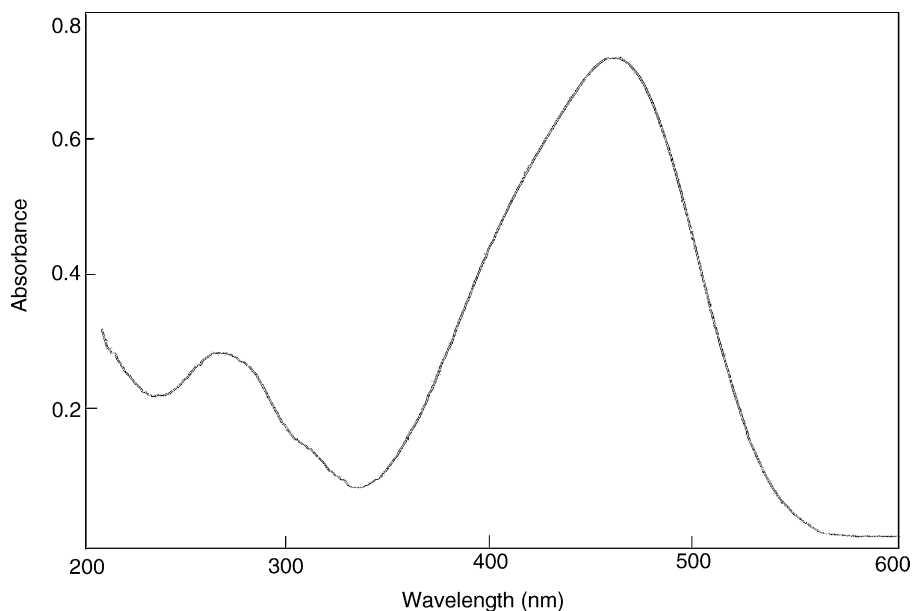
Fig. 2. The UV-Vis spectrum of methyl orange.

As shown in Fig. 3, the activity of the prepared sample increases with the increase of the catalytic concentration. When the concentration of the prepared catalysts was about 6 g/l, main part of the methyl orange in the solution can be degraded in 2 h. But further increasing of the catalyst concentration clearly decreases the activity of the prepared samples. These phenomena were presumed to the complete absorption of the light by a small portion of productive particles, while having many parasitic particles that compete on contaminants' adsorption but not on photons.

Fig. 4 shows the changes in the absorbance of aqueous methyl orange at 464 nm by the prepared sample as a function of UV irradiation time. As shown in
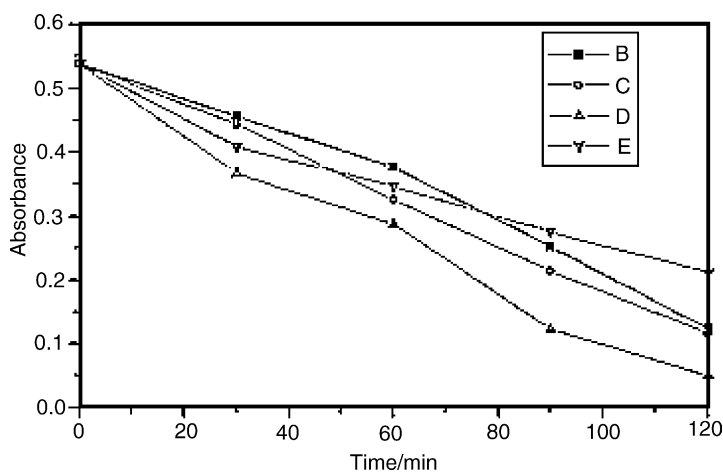

Fig. 3. The changes in absorbance of methyl orange solution at 464 nm by the prepared sample calcined at 600 °C as a function of UV irradiation time. The concentrations of the catalyst are (B) 4 g/l; (C) 5 g/l; (D) 6 g/l; (E) 7 g/l.
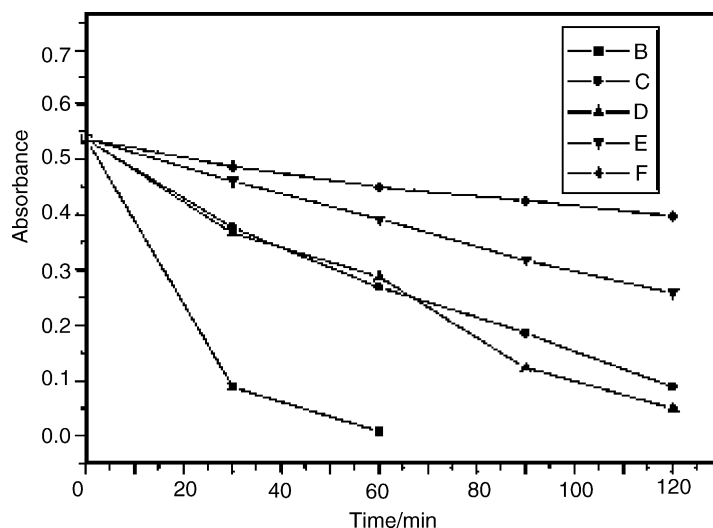
Fig. 4. The absorption spectra of methyl orange solution at different times following the photocatalystic degradation with the catalyst annealing at different temperature. The sintering temperature of the used catalysts are (B) 400 °C; (C) 500 °C; (D) 600 °C; (E) 750 °C; (F) 950 °C.

Fig. 4, the annealing temperature of the prepared samples has a great effect upon its ability to decolorize methyl orange solution. When using the catalysts calcined at 400 °C, after half an hour exposure in UV irradiation, the absorbance of methyl orange solution at 464 nm quickly changed from 0.538 to 0.089, which means the main part of the methyl orange in the solution had been degraded. As a composition, pure phase of anatase TiO_2 nanocrystals prepared by us need 2.5 h and the pure $Bi_4Ti_3O_{12}$ need 4 h to photodegrade 10 mg/l methyl orange solution completely under similar conditions. Yet the activity of

the prepared catalysts was shown decreased with the increase of the sintering temperature. When using the catalysts calcined at 950 °C for 10 min, as shown in Fig. 4, the absorbance of methyl orange solution at 464 nm decreased very slowly with reaction time. Photocatalytic decolorization of methyl orange is a pseudo-first-order reaction and its kinetics can be expressed as $\ln(A_0/A) = kt$ [13]. The calculated apparent reaction rate constants (k) of each catalyst from Fig. 4 are listed in Table 1. The different activity of each catalyst as shown in Table 1 is in accordance with the XRD patterns of the prepared

Table 1
Comparison of the apparent reaction rate constants calculated from Fig. 3 for each catalyst

Catalyst	Annealing temperature (°C)	Concentration (g/l)	Apparent reaction rate constants $(k/10^{-3}\ min^{-1})$	Methyl orange decolorization $(t_{1/2}/min)$[a]
1 at.% Zn-doped bismuth titanate	400	6	27.83	11
1 at.% Zn-doped bismuth titanate	500	6	5.437	55
1 at.% Zn-doped bismuth titanate	600	6	6.366	47
1 at.% Zn-doped bismuth titanate	750	6	2.412	125
1 at.% Zn-doped bismuth titanate	950	6	1.231	245
$Bi_4Ti_3O_{12}$[b]	650	6	2.45	122
Anatase TiO_2[c]	600	2	4.6	65

[a] Time required for 50% decolorization of 10 mg/l methyl orange solution.
[b] Pure anatase TiO_2 nanopowder and $Bi_4Ti_3O_{12}$ were also prepared by the CSD method under similar conditions.
[c] In our experiment 2 g/l anatase TiO_2 shows the highest activity to degrade the aqueous methyl orange.

samples. Photocatalytic properties of as-prepared Zn-doped bismuth titanates were drastically changed with the phase transition. The higher photocatalytic activity of the samples calcined at $400\,^{\circ}C$ is attributed to the $(Bi_{0.99}Zn_{0.01})_{20}TiO_{32}$ phase, which is presumed to have a high activity for the methyl orange. It can be confirmed that further increase of the annealing temperature to $600\,^{\circ}C$, when most $(Bi_{0.99}Zn_{0.01})_{20}TiO_{32}$ phase has been transformed into the $(Bi_{0.99}Zn_{0.01})_4Ti_3O_7$ phase as shown in Fig. 1, the prepared samples exposed a low photocatalytic activity. The origin for the higher photocatalytic property of $(Bi_{0.99}Zn_{0.01})_{20}TiO_{32}$ is not clear, further study of the properties of $(Bi_{0.99}Zn_{0.01})_{20}TiO_{32}$ is now in progress. As shown in Fig. 4 and Table 1, up to $750\,^{\circ}C$ when containing pure phases of $(Bi_{0.99}Zn_{0.01})_4Ti_3O_7$, the prepared samples showed lower activity compared with that of pure $Bi_4Ti_3O_{12}$ prepared by CSD method under similar conditions. Metal ion dopants influence the photoreactivity of catalysts by acting as electron (or hole) traps and by altering the e^-/h^+ pair recombination rate [11,12]. Although it is widely accepted that the photoreactivities of doped catalyst are related to the dopant trap site, it is more important that the trapped charges should be transferred to the interface to initiate the photoreactions. In dopants tested of TiO_2 crystals, Choi et al. [18] found an optimal dopant concentration of Fe^{3+} in TiO_2, the appearance of the optimal dopant concentration is attributed to the balance of an increase in trapping sites leading to efficient trapping and fewer trapped carriers leading to longer lifetimes for interfacial charge transfer. The observed photoreactivity decrease in $(Bi_{0.99}Zn_{0.01})_4Ti_3O_{12}$ is assumed to the large dopant concentration of Zn^{2+}, which leading to the dopants are more likely to serve as recombination centers than as trap sites for eventual charge transfer at the interface.

In summary, doping of bismuth titanate with 1 at.% Zn ions was prepared by the chemical solution decomposition method, and the phase transformation between $(Bi_{0.99}Zn_{0.01})_{20}TiO_{32}$ and $(Bi_{0.99}Zn_{0.01})_4Ti_3O_{12}$ was observed. Pure $(Bi_{0.99}Zn_{0.01})_{20}TiO_{32}$ was found showing a higher activity to photodegrade aqueous methyl orange than that of $(Bi_{0.99}Zn_{0.01})_4Ti_3O_{12}$.

Acknowledgements

References

[1] K. Honda, A. Fuhishima, Nature 238 (1972) 37.
[2] M.R. Hoffmann, S.T. Martin, W. Chi, D.W. Bahnemann, Chem. Rev. 95 (1995) 69.
[3] A.L. Linsebigler, G. Lu, J.T. Yates Jr., Chem. Rev. 95 (1995) 735.
[4] H. Yamashita, Y. Ichihashi, M. Anpo, M. Hashimoto, C. Louis, M. Che, J. Phys. Chem. 100 (1996) 16042.
[5] M. Anpo, Y. Ichihashi, M. Takeuchi, H. Yamashita, Res. Chem. Intermed. 24 (1998) 143.
[6] Z. Zhang, C.-C. Wang, R. Zakaria, J.Y. Ying, J. Phys. Chem. B. 102 (1998) 10871.
[7] J.F. Scott, C.A. Paz de Araujo, Science 246 (1989) 1400.
[8] P.C. Joshi, S.B. Desu, J. Appl. Phys. 80 (1996) 2349.
[9] S.C. Martin, C.L. Morrison, M.R. Hoffmann, J. Phys. Chem. 98 (1994) 13695.
[10] W. Choi, A. Termin, M.R. Hoffmann, J. phys. Chem. 98 (1994) 13669.
[11] M. Gratzel, R.F. Howe, J. Phys. Chem. 94 (1990) 2566.
[12] W. Mu, J.-M. Herrmann, P. Pichat, Catal. Lett. 3 (1989) 73.
[13] J.G. Yu, X.J. Zhao, Q.N. Zhao, Thin Solid Films 379 (2000) 7–14.
[14] D.W. Chen, A.K. Ray, Wat. Res. 32 (1998) 3223.
[15] Y. Hou, M. Wang, X.H. Xu, H. Wang, S.X. Shang, D. Wang, W.F. Yao, J. Crystal Growth 240 (2002) 489.
[16] H. Wang, L.W. Fu, S.X. Shang, X.L. Wang, M.H. Jiang, J. Phys. D: Appl. Phys. 27 (1994) 393.
[17] A.Q. Jiang, Z.X. Hu, L.D. Zhang, Appl. Phys. Lett. 74 (1999) 114.
[18] W. Choi, A. Termin, M.R. Hoffmann, J. Phys. Chem. 98 (1994) 13669.